High temperature elasticity and viscosity of GexSe1-x glasses in the transition range

Y. Gueguen, Tanguy Rouxel, Cédric Bernard, Vincent Keryvin, Jena-Christophe Sangleboeuf, Pascal Gadaud

Submitted to PRB July 14, 2010, revised Dec 22

High temperature elasticity and viscosity of Ge_xSe_{1-x} glasses in the glass transition range

Yann Gueguen[1)], Tanguy Rouxel[(1,€)], Pascal Gadaud[2)], Cedric Bernard[1)*], Vincent Keryvin[1)*], and Jean-Christophe Sangleboeuf [1)]

[1)]LARMAUR ERL-CNRS 6274, Université de Rennes 1, Bat. 10B, Campus de Beaulieu, 35042 Rennes cedex, France.

[2)]Laboratoire de Mécanique et Physique des Matériaux, CNRS UMR 6617, ENSMA, 1 Avenue Clément Ader, BP 40109, F-86961 Futuroscope Cedex, France.

[€)]Corresponding Author:

Tanguy Rouxel

Professor Tel: + 33-2-23236718

Fax: + 33-2-23236111

E-mail: tanguy.rouxel@univ-rennes1.fr

The viscous flow behavior and the temperature dependence of the elastic moduli of chalcogenide glasses from the germanium-selenium system were studied by means of homemade high temperature indentation setup and resonant frequency technique (1-10 kHz) respectively for temperatures between 0.8 and $1.2xT_g$. The softening rates, both in the elastic and in the viscous flow regimes, were correlated to network de-structuration or re-organization events in the light of previously reported high temperature neutron scattering data. The concomitant change of Poisson's ratio (ν) and the thermodynamics parameters of the thermally activated viscous flow process, were characterized and provide a new basis for the understanding of the sources for the softening in the transition range. The temperature dependence of ν suggests weak changes of the network cross-linking degree at large Ge-contents. On the contrary, in the case of a-Se a steep fragmentation of the structural units is inferred from the $\nu(T)$ data and the flow process is accompanied by a huge entropy change (activation entropy at saddle point). The entropy contribution at T_g ($T_g x \Delta S_a$) represents more than 50 % of the activation enthalpy for flow (ΔH_a) and increases with the selenium content. Hence the free activation energy (ΔG_a) is much smaller than apparent activation energy as derived from viscosity data.

I. INTRODUCTION

Glasses from the germanium-selenium system have already been extensively studied both because of their excellent transparency in the far infrared wavelengths range and because they show up as model binary covalent glasses[1-4]. However, the incidence of temperature on their properties is a critical issue, especially for the most chalcogen-rich compositions, which exhibit glass transition temperature below 350 K. It is of paramount interest not only at the processing and shaping stages, but also to evaluate the stability of glass parts in service conditions.

Elastic moduli are intimately related to volume density of energy (as expressed by the 1st Grüneisen rule[5]) and to the network connectivity. For instance Poisson's ratio was already found to correlate with the number of bridging oxygen atoms per Si-centered tetrahedron in silicate glasses[6] and to the network connectivity in general[7] and some linear relationships were proposed between ν and the average coordination number <n> (in the case of Ge_xSe_{1-x} glasses, $<n>=2(x+1)$)[8]. As far as <n> is less than 2.1, the selenium chains (or rings) are weakly interconnected so that deformation is expected to essentially proceeds through the alignment of the chains in shear planes. In this case properties are believed to be very sensitive to the weak inter-chains Van der Waals forces. A low shear resistance and a high Poisson's ratio follow. As <n> increases, covalent bonds come into play. At first sight, $<n>=2.4$ ($GeSe_4$ composition) corresponds to a complete cross-linking of Se and Ge layer units, two neighboring Ge atoms being separated by two Se atoms on average. At $<n>=2.67$ ($GeSe_2$ stoichiometry), homopolar Ge-Ge are present, and a tri-dimensional network is found, leading to a significant increase of the elastic moduli and of the viscosity[9], which can be viewed as a result of stressed rigidity[10]. The structure of these glasses might be slightly more complicated though, as will be further discussed, with Se occurring in at least three different sites[11] and possible "clustering" - at the scale of the structural units[12,13]. ^{77}Se experimental solid state Nuclear Magnetic Resonance and Raman scattering investigations have suggested a bimodal phase network, where the glass structure is composed of intertwined $GeSe_2$ and Se_n microdomains[14]. This assumption was based on the apparent absence of Se-Se-Ge fragments in the structure. Neutron-diffraction measurements and recent molecular dynamic simulations also suggests that the simple picture based on the <n> value is partially valid, as only about half of Se atoms are found in the predicted structural motifs[15,16]. The most recent studies imply that the structure a Ge-Se glasses significantly differs from the one predicted by the

simple chain-crossing and outrigger raft models[17], and very recent ^{77}Se NMR investigations evidence[18,19] the existence of Se-**Se**-Ge sites connecting $GeSe_2$ clusters and Se chains domains. However, whether the Ge-rich units are interconnected by means of Se chains (chain-crossing model) and whether Se form chains or rings (which size) are still matters of controversy. It is noteworthy that elastic moduli (continuum scale measurement) are essentially independent of the fine details of the network structure, provided the atomic coordination remains little affected. Nevertheless, the heterogeneous structure of the glass network at the molecular scale, with the possible coexistence of soft and stiff regions, will surely affect the temperature dependence through a "composite"-like effect which can be probed by means of high temperature measurements. Besides, elasticity data obtained in the temperature range for viscosity measurements allow for the derivation of the actual values for the activation energy and the free activation energy for flow from the directly available (apparent) eat of flow (enthalpy), as will be discussed further. The combination of elasticity and viscosity data provides thus a unique opportunity to get insight into the flow mechanisms and into the composition sensitivity of the rheological behavior.

II. MATERIALS AND EXPERIMENTAL METHODS

A. Materials

Ge_xSe_{1-x} glasses, with x between 0 and 0.3 were obtained from high purity elements Ge (99.9999%) and Se (99.999%). Se was further purified of remaining oxygen by the volatilization technique, consisting in heating Se at 523 K under vacuum for 2 hours. This method uses the greater vapor pressure of selenium oxide SeO_2 over that of the metal to remove the oxide species. Proper amounts of Ge and Se are subsequently introduced into an amorphous silica tube sealed in vacuum with a better than 10^{-2} Pa pressure in order to avoid oxygen contamination. The sealed silica tube was introduced into a rocking furnace and kept at 1023 K during 12 h to ensure a good mixing and homogenization of the liquid. The temperature was subsequently reduced to 923 K and staid constant for 1 h to reduce the gas pressure in the tube[3,12,13]. The obtained glass melt was then quenched in water (293 K) and annealed at T_g during 4 h to reduce the residual stresses resulting from the cooling. The glass rod was sliced and cut to the desired mechanical testing specimen geometry using a diamond saw. Surfaces of the specimens were mirror polished using SiC paper and alumina suspension (1/4 micron particle size).

The glass transition temperature T_g was measured by a TA Instrument differential scanning calorimeter DSC Q20, with a heating rate of 10 K/min, with a better than ±2 K accuracy.
The density was measured at 293 K using the Archimedes displacement technique using CCl_4. The variability of such a measurement is about ±0.5 %.

B. Experimental methods

Our laboratory has developed an equipment operating in the micro-indentation range, with applied loads between 0.01 and 15 N, consisting in a hot chamber equipped with an alumina tube and a sapphire indenter, and allowing for a better than 2 K accuracy along a 10 mm testing zone[20,21]. The whole equipment is situated in a vibration-free and air disturbance-free environment. The load is applied using a piezoelectric actuator and the penetration depth is measured with a capacitive sensor having a resolution of 10 nm. The load fluctuation is less than ± 12 mN. The maximum target temperature is 1473 K, with a thermal stability within 1 K variation up to 1323 K.
The shear viscosity coefficient (η) was estimated from indentation experiments performed at a constant load (P) of 1 to 12.5 N in air using a ball indenter (750 µm radius (R)) and is given by[21-23]:

$$\eta = \frac{3}{16}\frac{P}{\sqrt{R}}\left(\frac{d(u^{3/2}(t))}{dt}\right)^{-1}, \qquad (1)$$

where u is the penetration depth.
Recall that the viscous flow regime is associated to the stationary creep regime following the viscoelastic transient one. Consequently, the load was maintained long enough (typically 1 min above T_g to more than 1 hour for points recorded below T_g) to insure the occurrence of a stationary creep regime, as evidenced by a constant slope in the $u^{3/2}/P$ versus t curves. This problem is particularly critical as soon as measurements are carried out below T_g, i.e. in a range where the characteristic relaxation time increases rapidly and compares with the experimental duration. The specimen and the indentation set-up were kept at each testing temperature for up to 4 hours before loading to ensure a thermal equilibrium.

Young's modulus was determined by means of a resonant frequency technique in bending mode in the kHz range[24]. This method allows to perform experiments at 1 $K.mn^{-1}$ under high vacuum (10^{-4} Pa) up to 1300 K without any harmful contact, the sample beam

being maintained horizontally between steel wires located at the vibration nodes. Furthermore, excitation and detection are insured by an electrostatic device (capacitance created between the sample and a single electrode). The accuracy of this method is better than 0.5% for conducting bulk materials whatever the rigidity range. Young's modulus (*E*) is expressed as[24]:

$$E = 0.9464 \quad \rho F_B^2 \left[\frac{L^4(t)}{h^2} T(h/L, \quad \nu) \right], \tag{2}$$

where F_B is the resonance frequency in bending mode, ρ the specific mass, ν Poisson's ratio, h and L, the beam thickness and span length, and T(h/L,ν) a correcting factor close to 1.

For this work, 20×4×2 mm^3 parallelepipedic bars were plated on one face (AuPd metallic vapor deposition of about 10 nm thick) in order to be electrostatically excited.

A new testing head has been designed in agreement with ASTM recommendations to determine the shear modulus (μ) of plates (typically 30 mm × 12 mm × 1.5 mm) in torsion mode[25].

$$\mu = \frac{4\rho}{RL^2 F_T^2}, \tag{3}$$

where R is a shape factor equal to 17.51 in the present case, ρ is the specific mass, L is the length of the plate-like specimen and F_T is the torsion resonant frequency.

III. RESULTS

Owing to the experimental difficulty to assess high temperature elasticity data, and especially due to the machining of specimens in such brittle glasses (fracture toughness of GeSe glasses is typically below 0.3 $MPa.m^{0.5}$), measurements were limited to a-Se, $GeSe_4$, $GeSe_3$, and Ge_3Se_7 compositions (Fig. 1). Additional investigations focused on Young's modulus were previously reported by Gadaud et al.[24] for $Ge_{15}Se_{85}$ and Ge_3Se_7 compositions. The raw measurements of E, μ, and η are reported in Table I (note that these data might be further used to estimate the vibrational entropy of both the glass and the super-cooled liquids from the classical assumption that S_{vib} is proportional to $d\mu/dT$).

The elastic moduli exhibit only minor changes between room temperature (RT) and T_g. Their values at T_g are more than 80 % of their RT values. With regards to the considered temperature interval (0.8 to 1.1T_g) data in the super-cooled liquid region exhibit a linear dependence with temperature. The $\left.\frac{dE}{dT}\right|_{T \geq T_g}$ and $\left.\frac{d\mu}{dT}\right|_{T \geq T_g}$ slopes are reported together with the transition temperatures and the corresponding values of the elastic moduli in Table II. In all cases, experimental data exhibit a change of the softening rate in a temperature range corresponding within fifteen degrees to the glass transition temperature as obtained by classical means such as DSC and dilatometry. In the case of a-Se the transition observed in shear lies about 7 K below that observed in the E(T) curve. For reasons that have not been elucidated yet, the transition as observed from elasticity data is shifted to lower temperature, notwithstanding the fact that frequencies in the 1 to 10 kHz range were used. A similar observation on glasses from various systems and using a different experimental set-up was previously reported[7]. Nevertheless, since a clear transition between two regimes was always observed in a temperature range quite close to the one identified as the T_g range by DSC, this transition was considered in this work to be the glass transition range with respect to the used technique. The softening rate of a-Se above T_g (-115 MPa.K^{-1}) is close to the one reported for Zr-based metallic glasses[26] or oxynitride glasses[27], but is ~ twice less than that for glycerol (~ -190 MPa.K^{-1})[28]. The addition of germanium results in a significant reinforcement of the glass. With more than 25 at.% germanium, the softening rate (in absolute value) becomes 3 to 4 times smaller. The viscosity curves as obtained by instrumented indentation are plotted together with previously published data[29-33] on glasses with same compositions in Fig. 2a. The indentation method allows to cover a broad range of viscosity values on both sides of T_g, with a unique opportunity to probe the low temperature range associated with viscosities above 10^{13} Pa.s. It is noteworthy that the present data are in excellent agreement with those reported in the literature for $T>T_g$. There are 5 to 6 orders of magnitude differences in the viscosity coefficients at a given temperature between adjacent curved, i.e. as the germanium content changes by about 10 %.

In what follows, we will discuss the viscous flow process in the light of general concepts developed in the framework of thermally activated processes, regardless of any structural or microscopical ingredients. With regard to the viscosity range considered here - for η between 10^8 and 10^{15} Pa.s - the experimental data could be expressed with a smooth curve-fitting as a function of temperature using a classical Boltzmann term accounting for the probability of a given fluctuation to overcome the relevant energy barrier,

$$\eta = \eta_o \exp[\Delta G_a /(RT)] , \qquad (4)$$

where η_o is a temperature-independent factor, R is the perfect gas constant and ΔG_a is the free activation enthalpy for flow.

However, it must be emphasized that ΔG_a is by essence a temperature-dependent parameter (differentiation of the free enthalpy with respect to T is the negative of the entropy, so that the derivation of Eq.(4) with respect to temperature leads to:

$$R\left.\frac{\partial \ln \eta}{\partial(1/T)}\right|_\sigma = \Delta G_a - T\left.\frac{\partial \Delta G_a}{\partial T}\right|_\sigma = \Delta G_a - T\Delta S_a \qquad (5)$$

where σ is the stress applied on the specimen (see Refs [34],[35] for further background on this analysis) and is mentionned here to recall that T and σ are the two independent external variable in this problem.

By analogy with the formalism introduced in Chemical Kinetics[36], ΔS_a can be considered as the entropy of activation of the flow process. Hence, it is inferred from Eqs. (4,5) that the only directly available experimental parameter is the activation enthalpy (heat of flow),

$$\Delta H_a = R\left.\frac{\partial \ln \eta}{\partial(1/T)}\right|_\sigma , \qquad (6)$$

ΔH_a values as determined from the slope of the linear intercepts in Fig. 2b are reported in Table III. Following the classical theory of thermally activated flow phenomena, it is possible to estimate ΔG_a once the temperature dependence of the shear modulus is known (two important assumptions here are: i) the height of the energy barrier is proportional to the shear modulus, and ii) the contribution of the mechanical work to overcome the barrier is small in comparison to that of thermal activation)[34,35,37]:

$$\Delta G_a = \frac{\Delta H_a}{1 - \frac{T}{\mu}\frac{\partial \mu}{\partial T}} \qquad (7)$$

The activation entropy is then given by: $\Delta S_a = (\Delta H_a - \Delta G_a)/T$:

$$\Delta S_a = \frac{\frac{1}{\mu}\frac{\partial \mu}{\partial T}}{\frac{T}{\mu}\frac{\partial \mu}{\partial T} - 1}\ \Delta H_a \qquad (8)$$

Another approach was proposed by Nemilov[38], assuming that all viscosity curves meet in the supercooled liquid region at a given T_g/T ratio corresponding to a viscosity of about $10^{-4.5}$ Pa.s. In this latter approach both ΔG_a and ΔS_a are solely estimated from the viscosity data on the basis of Eqs. (5) and (6). For instance at T_g it comes that $\Delta S_a = -316 + \Delta H_a/T_g$ and $\Delta G_a(T_g) = 316 T_g$. The activation volume (V_a) associated to the overcoming (saddle point) of the energy barrier for flow is another important parameter. Since $V_a = -\left.\frac{\partial \Delta G_a}{\partial \sigma}\right|_T$, it is in principal required to perform temperature jump experiments for different values of the applied stress to estimate the activation volume. However Nemilov[39] proposed a simple estimation for a volume V*, considered to be that of kinetic units overcoming the activation barrier, from the free activation enthalpy for flow and from the shear modulus, $V^* = \Delta G_a/\mu$, and concluded that V*/N (N: Avogadro number) can be written as r_o^3 where r_o is in excellent agreement (within 10 %) with some interatomic distance (see ref. [35] for details). A similar expression was obtained by Dyre et al.[40] using a volume expansion model, although in this later case the characteristic volume was given a slightly different meaning.

The values for the parameters of the thermally activated viscous flow process are reported in Table III.

IV. DISCUSSION

The softening of glasses above T_g is chiefly related to the destructuration of the atomic network. However, the microscopic events at the source for this thermal weakening are quite complicated and differ from one glass to the other. Various scenarios might be invoked depending on the type of structural units and on the inter-units bonding. Generally speaking, the whole network topology comes into play. Interestingly, elastic moduli and shear viscosity coefficient are likely to be primarily sensitive to different microscopic features. For instance, Young's modulus is likely to be affected by the stiffness of the structural units to a normal

stress, whereas the shear modulus is more sensitive to the inter-unit bonding. In principle, elastic moduli are little affected by the size or the length of the structural units (recall that neither the shape nor the size of the phases affect the moduli of a composite mixture; Only the respective volume fractions matter), as far as there is no dramatic structural changes. On the contrary, viscosity is very sensitive to the size and shape of the structural units and to the presence – or absence - of a continuous softer phase. In what follows, we intend to get insight into the softening mechanisms in the light of the abundant literature published on the structure of germanium selenide glasses and on the thermally induced structural changes.

A. Network cross-linking, average coordination and elastic behavior

The increase of both E and μ with the germanium content mainly stems from the increase of <n>. Bridges[6] and Nemilov[39] reported some interesting correlation between Poisson's ratio (ν) and glass network structures, and ν was found recently to show up as a remarkable index of the cross-linking degree, regardless of the chemical system[7]. For Ge_xSe_{1-x} glasses, a linear relationship (correlation=0.985) is obtained from previously published elasticity data on the same specimens[41]:

$$\nu=0.5135-0.0946\langle n\rangle \qquad (9)$$

Where <n> is the average coordination number. Note that a very close relationship was also reported in the Ge-Sb-Se system[8].

Although E, μ, and ν change monotonically with <n> , their temperature dependences are more interesting. For instance, both dE/dT and dμ/dT (table II) are larger for the $GeSe_3$ composition, in the supercooled liquid range (T_g^+), than for the $GeSe_4$ and Ge_3Se_7 compositions. It is noteworthy that the $GeSe_3$ composition precisely lies in the so-called intermediate phase range (after Boolchand et al.[10,42]).

Although it receives little attention so far, the temperature dependence of ν is of paramount interest to probe the thermally induced structural changes in the cross-linking. Recalling that $\nu=E/2\mu-1$, ν(T) data were calculated from E(T) and μ(T) ones (Fig. 3). A perfectly incompressible body is characterized by ν=0.5 and rubber, glycerol and Pd-based metallic glasses get very close to this upper bound above their T_g. On the contrary, a-SiO_2 (a tetrahedrally coordinated glass as $GeSe_2$) retains its cross-linked structure well beyond the T_g

range[7]. In the present case it seems that the cross-linking remains strong in both $GeSe_3$ and Ge_3Se_7 compositions up to $1.1xT_g$ whereas a-Se experiences a severe depolymerization and approaches the liquid state in a steep manner. It is noteworthy that for a-Se the increase of ν begins below the T_g range as estimated from E(T) curves. A similar temperature shift was reported earlier on a-Se by Böhmer et al.[9] from ultrasonic investigations in the 1-20 MHz range. The excitation frequencies used here are close to 5 and 8 kHz and the corresponding periods ($1\text{-}2\ 10^{-4}$ s) are thus hundreds of times smaller than the characteristic relaxation time (η/μ from the Maxwell model), which is larger than 5 min below T_g. Therefore it doesn't seem reasonable to invoke any dynamic effect, in accord with Böhmer's conclusion[9], nor to account for the dynamic Poisson's ratio[43]. A possible explanation is that the weak inter-chain bonding (major contribution to μ) collapses at a lower temperature than the covalent bonds. The fragmentation of the chains may also weaken the shear resistance more than the uniaxial stiffness. However, the elasticity measurements on a-Se should be taken with caution for the following reasons: i) Dynamic structural relaxation might occur during loading due to a T_g range close to ambient temperature; and ii) The ± 2 K accuracy of our equipment might be a problem for the calculation of ν of low T_g glasses, because small temperature differences induce large changes in E and μ, leading to a dramatic deviation in ν.

Now, let us summarize what we can learn from the literature about thermally induced structural changes in the studied glasses. a-Se is often considered to consist of a mixture of chain and ring units, with an expected decrease of the amount of rings with rising temperature above T_g[44,45]. Dembovsky[46] concluded from quantum chemical data that in addition to 2-fold coordinated atoms there was a growing number with rising temperature of 4-fold coordinated Se (over 10 % at T_g). It was suggested that this could play a role in the high temperature range (for $T/T_g<1.3$[46,47]), higher than the temperature range of interest in this study. It has also been concluded from small angle neutron scattering that the chain macromolecules of a-Se, consisting of 10^4 to 10^6 atoms, up to T_g[42], shorten upon increasing temperature in the liquid range[45,49]. Rings are very likely to give a significant contribution to the resistance opposed to transverse contraction when the material is pulled in tension (recall that foams or cellular solids exhibit very low values for Poisson's ratio). Hence, the disappearance of rings is supposed to be of paramount importance on the increase in ν. The site fraction of Se atoms building rings was estimated to lie about 0.85, 0.78, 0.66 and 0.56 at 293, 300, 350 and 400 K respectively[45]. It is inferred from the abrupt increase in Poisson's ratio that this destructuration is very rapid within 10 K around T_g; and the fraction of ring in this

temperature range can not be considered as resulting from a percolation of these units[50,51]. Now, because the inter-chain bonding is relatively weak (Van der Waals type), upon heating a-Se looks more and more like short $(\text{-Se-})_n$ segments embedded in a soft phase, so that shear is enhanced and both shear modulus and viscosity drop sharply.

The introduction of germanium adds to the complexity of the problem. When the selenium content exceeds 80 % ($GeSe_4$, $GeSe_9$) anomalous wide angle X-ray scattering and small angle X-ray scattering suggest that the structure is mainly constituted by isolated $GeSe_4$ tetrahedra in an amorphous Se matrix[12]. A recent first principle molecular dynamics simulation on $GeSe_4$ proposes more details to the picture: 88% of Ge atoms are involved in tetrahedral $GeSe_4$ units and a few are not four-fold coordinated to Se, but would form $Ge\text{-}Se_2$ and $Ge\text{-}GeSe_3$ units, while Se would form $Se\text{-}Se_2$, Se-Se-Ge, and $Se\text{-}Ge_2$ motifs[16]. At lower selenium content, corner-sharing and edge-sharing tetrahedra are observed[12,18]. This suggests, that there are few – or less[17-19] than expected from the stoichiometry (chain-crossing model) -Se-Se bridges between $GeSe_{4/2}$ tetrahedra, even for the $GeSe_4$ composition. This indicates the presence of Se-rich units in the structure, but not isolated, as suggested by the bimodal model. In addition, due to the relative ease for the dissociation of $GeSe_2$ units[52], it is anticipated that more and more homopolar bonds (Ge-Ge, Se-Se) will form upon heating above T_g, giving to the network a more and more chemically heterogeneous nature. Neutron Scattering studies[53,54] conducted on liquid samples from the Ge_xSe_{1-x} system at temperature above 900 K confirmed the disappearance of heteropolar Ge-Se bonds with increasing temperature in the liquid range and indicate that the intermediate range order becomes less significant while the average coordination number <n> does not seem to change. Besides, although weak regions develop in the glass network, $GeSe_{4/2}$ tetrahedral units are not much affected. These units clearly oppose to transverse contraction under tensile loading and are responsible for a relatively low value and for a weak temperature sensitivity of ν in the presence of significant amount of germanium. Our $\nu(T)$ data also suggest little change in the network cross-linking degree in the case of $GeSe_3$, $GeSe_4$ and Ge_3Se_7 compositions and are thus consistent with these structural observations. ***Furthermore, the fact that $GeSe_3$ and $GeSe_4$ compositions behave very similarly (normalized elasticity and viscosity curves are almost superimposed), would support either the existence of an intermediate phase controlling the behavior in this composition range (x=0.2 to 0.25)[55], or the possibility that for Ge content over 20 at%, the Se-rich are progressively taking over the $GeSe_2$ units in controlling the properties of the glasses. This is in agreement with a recent ^{77}Se NMR study[56] suggesting few bond exchanges between Se rich domains and $GeSe_2$ units, and larger mobility of Se-Se-Se sites.***

B. Thermal activation parameters and deformation mechanism

The height of the free activation energy, ΔG_a, for the viscous flow process is much lower than any interatomic bonding energy (264, 330 and 484 kJ.mol^{-1} for U_{oGe-Ge}, U_{oSe-Se} and U_{oSe-Ge} respectively[51]). This suggests that deformation proceeds by shear along the soft regions in-between stiffer structural units. The larger the selenium content is and the larger the activation entropy (ΔS_a) induced by the flow process and the fragility index (m) become (Fig. 4 and Table II). This is in agreement with the work published by Nemilov[38], which already suggested a strong correlation between ΔS_a and m. As long as stress effects on viscosity can be neglected (i.e. flow remains Newtonian), ΔS_a reflects the temperature dependence of the energy barrier and is chiefly related to thermally induced changes of the shear modulus (see Eq. (7)). Therefore the large entropy contribution and the abrupt entropy change above T_g (Fig. 5) in the case of a-Se corroborates the steep softening observed in the same temperature range.

Amorphous selenium: There are obviously some dramatic microscopic events responsible of the rapid softening and increase of the activation entropy at T_g. Misawa et al.[45] studied the temperature dependence and the energetics of the ring to chain transition in a-Se. In particular these authors intended to estimate the entropy increase associated with the fragmentation of the Se chains. The following expression was derived for the entropy increase:

$$\Delta S = R \ln\left[\left(\frac{n_c}{q}\right)^q \frac{1}{f_c^{2q-1}\,(q-1)!\,\xi^q}\right], \qquad (10)$$

where n_c is the number of Se atoms in the chain before fragmentation and q is the number of Se-Se bond disruptions (n_c/q: average number of atoms in the fragments), f_c is the fraction of chains (versus rings) and ξ is a constant calculated to be $4.2.10^{-3}$. Using their data at T_g ($n_c/q \sim 5.10^5$, $f_c \sim 0.22$) an entropy change of ~1100 J.mol^{-1}.K^{-1} (Fig. 5) would correspond to 6 cuts in a chain. At 350 K ($T/T_g \sim 1.12$), with $n_c/q \sim 2.10^5$ and $f_c \sim 0.34$, the same entropy change corresponds to 8 cuts. Just below T_g, the number of cut falls down to about 4 (ΔS=700 J.mol^{-1}.K^{-1}, $n_c/q \sim 10^6$, $f_c \sim 0.15$). It would be very interesting to study the changes of the chain length and chains to rings fraction in situ at high temperature under stress to determine whether

viscous flow affects these processes or not. At higher temperature the activation entropy is expected to decrease as the system gains more and more ergodicity. This is indeed predicted by Eq. (8): As T increases and μ decreases toward zero, ΔS_a tends toward 1/T. It is noteworthy that glasses such as glycerol and selenium consisting of chain-like structural units experience a large change in ΔS_a in the transition range, whereas weak changes are observed in more cross-linked glasses, such as a-SiO_2.

Germanium selenide glasses: We observed a decrease of the temperature sensitivity of the viscosity (ΔH_a) with an increase of the germanium content up to 20 % ($GeSe_4$). Then ΔH_a increases and reaches a value for Ge_3Se_7 higher than for $GeSe_9$. Our data corroborate previously reported data on similar glasses[30,54] and which concluded to a U-shape curve for ΔH_a as a function of the germanium content, with a decrease for <n> below 2.4 and an increase above this value and up to the $GeSe_2$ composition. The activation energy for enthalpy relaxation shows also an identical U-shape[14]. However one should keep in mind that the free activation enthalpy ΔG_a is the relevant parameter of the flow process and is systematically smaller than the apparent energy, ΔH_a. The discrepancy is especially large for a-Se (41 $kJ.mol^{-1}$ and 369 $kJ.mol^{-1}$ for ΔG_a and ΔH_a respectively). A monotonic increase of ΔG_a with the germanium content, from 95 $kJ.mol^{-1}$ for a-Se to 183 $kJ.mol^{-1}$ for Ge_3Se_7, is predicted from the simple model proposed by Nemilov[38]. These values are in reasonable agreement with those we obtained taking advantage of our high temperature elasticity data (41 $kJ.mol^{-1}$and 145 $kJ.mol^{-1}$ respectively). This monotonic trend might simply reflect the fact that an increase of the germanium content results in an increase of the elastic moduli and thus to an increase of the volume density of energy (1^{st} Grüneisen rule). The height of the energy barrier for viscous flow being of an overwhelming part of elastic origin, a monotonic increase of ΔG_a with the germanium concentration follows. Therefore, the unexpected U-shape curve depicted by ΔH_a as a function of the germanium content is simply due to a dramatic composition-dependence of the activation entropy. The relatively strong temperature sensitivity of the viscosity at large germanium contents, with a fragility index remaining as large as 27 for both $GeSe_3$ and Ge_3Se_7, stems from the fact that the breakdown of the cross-linked network structure (disappearance of the medium range order) above T_g favors shear in-between structural units, which are no more strongly interconnected, so that the microscopic events which cause viscous flow are likely to be very similar in all cases. Eventually, glasses containing at least 40 % germanium (Ge_2Se_3) are likely to consist of Ge-rich clusters in a selenium matrix and might show a fragility index close to the one of pure a-Se, as observed

by Senapati et al.[32] Our understanding of the incidence of the composition and structure of germanium selenide glasses on their elastic and viscous deformation is illustrated by the schematic drawings depicted in Fig. 6 and corresponding to the following situations: a) In glassy selenium 8-member rings chiefly predominate over chains. When the temperature approaches the transition range (Fig. 6b) rings progressively disappear to the benefit of chains and Poisson's ratio starts to increase due to the loss of the resistance against transverse shrinkage. Above the transition the fragmentation of the chains becomes more and more significant and some alignment of the fragments may be observed (Fig. 6c). The higher the temperature becomes and the smaller the fraction of rings and the number of atoms per Se chains (Fig. 6d) are. The addition of germanium results in the formation of relatively rigid $GeSe_{4/2}$ tetrahedra. As far as the germanium content remains below 20 at.%, the glass network exhibits weak selenium-rich path for shear in-between Ge-based tetrahedra. The glass network shows up like $GeSe_{4/2}$ tetrahedra clusters with few connections with a soft amorphous selenium matrix (Fig. 6e). When the germanium content is high enough, say for $x \geq 0.20$ ($GeSe_4$), a subnetwork of interconnected tetrahedra forms which brings stiffness to the glass (Fig. 6f). At germanium content over 25 at.% ($GeSe_3$), the cross-linked network provides numerous transverse stressed arms, likely to follow edge-sharing tetrahedra. Hence Poisson's ratio turns out to be quite small and to evolve little with temperature through the transition range. It is noteworthy however than in spite of a highly cross-linked network, there still remain some continuous channels between edge-shared $GeSe_{4/2}$ tetrahedra, which provide paths for the shear deformation (Fig. 6h). Moreover, increasing the temperature could increase the ratio of edge-shared tetrahedra, allowing such weak channels to extend[58]. Edwards et al.[58] even suggest that the corner to edge sharing transition could be the main process involved during shear flow and enthalpy relaxation, because these three processes have similar characteristic relaxation times. Nevertheless, these two latter should involve different structural events, as it is evidenced by their apparent activation energies (~110 kJ/mol for enthalpy relaxation[14], 243 kJ/mol for shear flow, for $GeSe_4$ – table III-). With rising temperature, Ge-rich and Se-rich regions have the tendency to form (a growing amount of homopolar Ge-Ge and Se-Se bonds are found with increasing temperature in liquid $GeSe_2$[52]) due to the ease for dissociation of $GeSe_2$. Thus the shear viscosity drops. The activation volumes (Table III) suggest volumes corresponding to a single atom for a-Se and few atoms for $GeSe_3$ and Ge_3Se_7. These values are certainly no more than rough indications due to the simplistic model used for their estimation. Nevertheless, they support the idea that

the relevant scale for flow is typically the chain link in the case of a-Se and the size of the tetrahedron when $GeSe_{4/2}$ units come into play.

V. SUMMARY AND PERSPECTIVES

We have studied the high temperature elastic behavior and the shear viscosity of germanium selenide glasses in the transition range. Young's modulus and the shear modulus were measured by means of a resonant technique in the 5 to 10 kHz range. Viscosity was measured using a displacement- and load-controlled indentation apparatus. A steep increase in Poisson's ratio (ν) starting slightly below T_g was observed for a-Se whereas little changes were noticed for $GeSe_3$ and $GeSe_7$ compositions. Since ν was found previously in a couple of independent works[6-8] to be directly correlated to the network cross-linking degree, and to the mean coordination number in chalcogenide glasses, our results strongly suggest that over-constrained Ge-Se glasses experience minor structural changes in the transition range.

The viscous flow behavior could be well described by a pure Arrhenius-type law with a single apparent activation energy, ΔH_a, for the flow process in the temperature range of concern (0.8 to $1.1T_g$). The estimated values for ΔH_a are in good agreement with those reported by previous investigators in the same temperature range and show a constant decrease with rising Ge content up to 20 at% Ge, that correlate with a minimum in reported heat flows at the glass transition. However for higher Ge contents, ΔH_a increases. We have applied the theory of thermally activated flow phenomena to analyze our data and derive the activation entropy for flow by means of both elasticity and viscosity data. It turns out that the activation entropy is very high for a-Se and decreases rapidly with rising Ge content. Consequently, the free enthalpy of the flow process is in fact much lower that ΔH_a for the Se-rich compositions. We propose that the entropy change is of an overwhelming part of elasticity origin and is intimately related to the fragmentation of the chains and probably to a lesser extent to the ring to chain transition. A sketch of the different events occurring in the studied glasses was drawn to describe the structural changes and the deformation mechanisms as a function of the composition. In particular special focus was made to explain the occurrence of easy shear zones in over-constrained Ge-Se compositions, notwithstanding the weak changes of ν observed in the same temperature range.

Most structural studies on germanium chalcogenide glasses were performed either at room temperature or in the liquid range for $T>>T_g$. We feel that X-ray and neutron scattering conducted in situ in the transition range under stresses would be invaluable to get insight into

the stress-induced structural changes and thus into the deformation process. For instance this would allow estimating possible effects of the stress on the characteristics of the structural units (namely the Se-chains conformation and length, the inter- and intra-tetrahedral angles, the texturation etc.).

ACKNOWLEDGMENTS

We are indebted to Dr. Q. Coulombier and to the UMR CNRS 6226 for providing us with high quality melt-quenched chalcogenide specimens respectively. We are also grateful to all the people at LARMAUR who offered their valuable help to the experimental investigations. This work has been partly supported by the French Ministry of Higher Education and Research (Ph-D grant for Yann Gueguen). We also wish to thank Prof. S.V. Nemilov (St. Petersburg State University of Information Technologies, Mechanics and Optics, St Petersburg, Russia), Prof. P. Salmon (University of Bath, GB) for their helpful remarks on the manuscript.

---

* Present address: LIMATB, EA-4250, UBS-LORIENT, Centre de Recherche, rue de Saint Maudé - BP92116, 56321 Lorient cedex, France.

1. J.A. Savage, “Infrared optical materials and their antireflection coating”, Ed Adam Higlger (1985).
2. J. Portier, "Halogenide, chalcogenide and chalcohalogenide glasses: materials, models, applications", J. Non-Cryst. Sol. **112** [1-3], 15-22 (1989).
3. J. Lucas, "Halide Glasses", in "Glasses and amorphous materials", Ed. J. Zarzycki, ch. 8 557-488, Pub. VCH (New-York) (1991).
4. A.K. Varshneya, Fundamentals of Inorganic Glasses, Academic Press Inc. (Boston, London, Tokyo), p. 7 (1994).
5. Grüneisen 1st rule in "Physical Properties of Solid Materials", Ed. C. Zwikker, Willey Interscience, New-York, p.90 (1954).
6. B. Bridge and A.A. Higazy, "A model of the compositional dependence of the elastic moduli of multicomponent oxide glasses", Phys. Chem. Glasses **27** [1], 1-14 (1986).
7. T. Rouxel, “Elastic properties and short-to-medium range order in glasses”, J. Am. Ceram. Soc. **90** [10], 3019-3039 (2007).

8. A.N. Sreeram, A.K. Varshneya, D.R. Swiler, « Molar volume and elastic properties of multicomponent chalcogenide glasses », J. Non-Cryst. Sol. **128**, 294-309 (1991).
9. R. Böhmer, and C.A. Angell, « Elastic and viscoelastic properties of amorphous selenium and identification of the phase transition between ring and chain structures », Phys. Rev. B **48** [9], 5857-5863 (1993).
10. P. Boolchand, X. Feng, and W. J. Bresser, "Rigidity transitions in binary Ge-Se glasses and the intermediate phase", J. Non-Cryst. Solids **293 – 295**, 348 (2001).
11. C. Massobrio, M. Micoulaut, P.S. Salmon, "Impact of the exchange-correlation functional on the structure of glassy $GeSe_2$", Solid State Sciences **12**, 199-203 (2010).
12. P. Armand, A. Ibanez, H. Dexpert, D. Bittencourt, D. Raoux, and E. Philippot, « Structural Approach of Ge-X, GeX_2-Ag_2X (X=S, Se) Glassy systems », J. Phys IV **C2**, 189-194 (1992).
13. B. Bureau, J. Troles, M. Le Floch, P. Guenot, F. Smektala and J. Lucas, "Germanium selenide glass structures studied by ^{77}Se solid state NMR and mass spectroscopy", J. Non-Cryst. Solids **319**, 145-153 (2003).
14. P. Lucas, E.A. king, O. Gulbiten, J.L. Yarger, E. Soignard, and B. Bureau, "Bimodal phase percolation model for the structure of Ge-Se glasses and the existence of the intermediate phase", Phys. Rev. B 80, 214114 (2009).
15. I. T. Penfold and P. S. Salmon, "Structure of covalently bonded glass-forming melts: A full partial-structure-factor analysis of liquids $GeSe_2$", Phys. Rev. Lett. **67**, 97 1991.
16. C. Massobrio, M. Celino, P.S. Salmon, R.A. Martin, M. Micoulaut, and A. Pasquarello, "Atomic structure of the two intermediate phase glasses $SiSe_4$ and $GeSe_4$", Phys. Rev. B **79**, 174201 (2009).
17. R. Golovchak, O. Shpotyuk, A. Kozyukhin, A. Miller, and H. Jain, "Structural paradigm of Se-rich Ge-Se glasses by high-resolution x-ray photoelectron spectroscopy", J. Appl. Phys, **105**, 103704 (2009)
18. E. Gjersing, S. Sen and B. Aitken, "Connectivity and configurational entropy of Ge_xSe_{1-x} glasses : Results from ^{77}Se MAS NMR spectroscopy", J. Phys. Chem. **114**, 8601-8608 (2010)
19. M. Kibalchenko, R.J. Yates, C. Massobrio and A. Pasquarello, "Structural Composition of First-Neighbor Shells in $GeSe_2$ and $GeSe_4$ Glasses from a First-Principles Analysis of NMR Chemical Shifts", J. Phys. Chem., in Press (2011)
20. Bernard, C. « Indentation et rhéologie de verres organiques de 20 a 700°C », *Ph.D thesis, University of Rennes 1* (2006).

21. C. Bernard, V. Keryvin, J.-C. Sangleboeuf, and T. Rouxel, « Indentation creep of window glass around the glass transition », Mech. of Mat. **42**, 196-206 (2010).
22. Ting, T. C. T. Contact Stresses between a Rigid Indenter and a Viscoelastic Half-Space. J Appl. Mech. **33**, 845-& (1966).
23. Sakai, M. & Shimizu, S. Indentation rheometry for glass-forming materials. J. Non-Cryst. Solids **282**, 236-247 (2001).
24. P. Gadaud, and S. Pautrot, « Characterization of the elasticity and anelasticity of bulk glasses by dynamical subresonant techniques », J. Non-Cryst. Sol. **316**, 146-152 (2003).
25. P. Gadaud, X. Milhet, and S. Pautrot, « Bulk and coated materials shear modulus determination by means of torsional resonant method », Mat. Sci. Eng. A **521-522**, 303-306 (2009).
26. V. Keryvin, T. Rouxel, M. Huger, and L. Charleux, "Elastic moduli of a ZrCuAlNi bulk metallic glass from room temperature to complete crystallisation by in situ pulse-echo ultrasonic echography", J Ceram. Soc. Japan **116** [1356], 851-854 (2008).
27. T. Rouxel, J-C. Sanglebœuf, M. Huger, C. Gault and S. Testu, "Temperature dependence of Young's modulus in Si_3N_4-based ceramics: roles of sintering additives and of SiC-particle content", Acta Mat. **50**, 1669-1682 (2002).
28. W.M. Slie, A.R. Donfor, and T.A. Litovitz, "Ultrasonic shear and longitudinal measurements in aqueous glycerol", The Journal of Chem. Phys. **44** [10], 3712-3718 (1966).
29. S.V. Nemilov, Viscosity and structure in glasses in the selenium–germanium system, Z. Prikl. Khim. **37**, 1020 (1964).
30. R.B. Stephens, « The viscosity and structural relaxation rate of evaporated amorphous selenium », J. Appl. Phys. **49** [12], 5855-5863 (1978).
31. W.H. Poisl, W.C. Olivier, and B.D. Fabes, " The relationship between indentation and uniaxial creep in amorphous selenium », J. Mat. Res. **10** [8], 2024-2032 (1995).
32. U. Senapati, and A.K. Varshneya, " Viscosity of chalcogenide glass-forming liquids : an anomaly in the 'strong' and 'fragile' classification ", J. Non-Cryst. Sol. **197**, 210-218 (1996).
33. F.Q. Yang, and J.C.M. Li, " Viscosity of selenium measured by impression test ", J. Non-Cryst. Sol. **212**, 136-142 (1997).
34. G. Schoeck, " The Activation Energy of Dislocation Movement ", Phys. Stat. Sol. B **8** [2], 499-507 (1965).

35. A. G. Evans, R. D. Rawlings, " The Thermally Activated Deformation of Crystalline Materials ", Physica Status Sol. B **34** [1], 9-31 (1969).
36. V. K. La Mer, "Chemical Kinetics. The temperature dependence of the energy of activation. The entropy and free energy of activation", The J. of Chem. Phys. **1** [5], 289-296 (1933).
37. B. Escaig, and J.M. Lefebvre, "Thermodynamic and kinetic analysis of non elastic deformation in polymeric glasses ", Rev. Phys. Appl. **13** [6], 285-292 (1978).
38. S. Nemilov, " Review : Structural aspect of possible interrelation between fragility (length) of glass forming melts and Poisson's ratio of glasses ", J. Non-Cryst. Sol. **353**, 4613-4632 (2007).
39. S.V. Nemilov, " Interrelation between shear modulus and the molecular parameters of viscous flow for glass forming liquids ", J. Non-Cryst. Sol. 352, 2715-2725 (2006). See also: ibid. in "Thermodynamics and Kinetic Aspects of the vitreous State", CRC, Boca Raton, 1995.
40. J.C. Dyre, N.B. Olsen, and T. Christensen, "Local elastic expansion model for viscous-flow activation energies of glass-forming molecular liquids", Phys. Rev. B **53** [5], 2171-2174 (1996).
41. J-P. Guin, T. Rouxel, J-C. Sangleboeuf, I. Melscoët and J. Lucas, "Hardness, toughness and scratchability of Ge-Se chalcogenide glasses", J. Am. Ceram. Soc. **85**, 1545-1552 (2002).
42. X. Feng, W.J. Bresser, and P. Boolchand, "Direct Evidence for Stiffness Threshold in Chalcogenide Glasses", Phys. Rev. Lett. **78**, 4422 (1997).
43. Tschoegl, N. W., Knauss, W. G. & Emri, I. Poisson's ratio in linear viscoelasticity - A critical review. Mech Time-Depend Mat. **6**, 3-51 (2002).
44. A.V. Tobolsky, and A. Eisenberg, " Equilibrium polymerization of sulfur ", J. Am. Chem. Soc. **81**, 780-782 (1959)
45. M. Misawa, and K. Suzuki, "Ring-chain transition in liquid selenium by a disordered chain model", J. Phys. Soc. Japan **44** [5], 1612-1618 (1978).
46. S.A. Dembovsky, "New sight into the structure of selenium: Four-valence Se in glass", J. Non-Cryst. Sol. **353**, 2944-2948 (2007).
47. S. Hamada, N. Yoshida, and T. Shirai, " On the viscosity of liquid selenium ", Bull. Chem. Soc. Japan **42**, [4] 1025-1029 (1969).
48. C.A. Angell, " Relaxation in liquids, polymers and plastic crystals – strong/fragile patterns and problems ", J. Non-Cryst. Sol. **131-133**, 13-31 (1991).

49. M. Inui, S. Takeda, K. Maruyama, Y. Kawakita, S. Tamaki, and M. Imai, " SANS measurements of liquid and amorphous selenium ", Physica B **213&214**, 552-554 (1995).
50. For instance, identifying the 8-member selenium rings to overlapping oblate ellipsoids with aspect ratios between 1/3 and 1/5 (which is roughly the width to diameter ratio of the rings according to structural studies), a percolation threshold between 0.17 and 0.23 is predicted following the theoretical analysis reported by Garboczi et al. (see Ref. [40]). It can be inferred from a study on sulphur that the fraction of chalcogen atoms involved in rings in the temperature range where the onset of the increase of Poisson's ratio is observed is about 0.74-0.78 (see Ref. [33]), i.e. still much larger than the percolation threshold. The difference would be even greater with the assumption of non-overlapping objects and would still be significant if spheres would have been considered instead of ellipsoids.
51. E.J. Garboczi, K.A. Snyder, J.F. Douglas, and M.F. Thorpe, " Geometrical percolation threshold of overlapping ellipsoids ", Phys. Rev. E **52** [1], 819-828 (1995).
52. P.A.G. O'Hare, and A. Zywrinsky, " Thermodynamics of (germanium + selenium). A review and critical assessment ", J. Chem. Thermod. **28**, 459-480 (1996).
53. K. Maruyama, M. Inui, S. Takeda, S. Tamaki, Y. Kawakita, " Neutron scattering studies on liquid Ge-Se mixtures ", Physica B **213&214**, 558-560 (1995).
54. P. S. Salmon, " Structure of liquids and glasses in the Ge-Se binary system ", J. Non-Cryst. Sol. **353**, 2959-2974 (2007).
55. M. Micoulaut and J.C. Phillips, "Onset of rigidity in glasses: from random to self-organized networks", J. of Non-Cryst. Solids **353**,1732-1740 (2007).
56. E.L Gjersing, S. Sen and R.E. Youngman, "Mechanistic understanding of the effect of rigidity percolation on structural relaxation in supercooled germanium selenide liquids", Phys. Rev. B 82, 014203 (2010).
57. V.M. Glazov, O.V. Situlina, Doklady Chemistry **187**, 587 (1969).
58. T. Edwards and S. Sen "Structure and Relaxation in Germanium Selenide Glasses and Supercooled Liquids: A Raman Spectroscopic Study", J. Chem. Phys. B, **115**, 4307 (2011).

TABLE I. Measurements of elastic moduli and shear viscosity coefficient as a function of temperature. x: Non-measured.[1)]as determined from the E(T) curves (Table II).

	a-Se Tg=302 K			$GeSe_4$ Tg=416 K			$GeSe_3$ Tg=498 K			Ge_3Se_7 Tg=579 K		
T/T_g [1)]	E (GPa)	μ (GPa)	$\log_{10}$ | (Pa.s)	E (GPa)	μ (GPa)	$\log_{10}$ η (Pa.s)	E (GPa)	μ (GPa)	$\log_{10}$ η (Pa.s)	E (GPa)	μ (GPa)	$\log_{10}$ η (Pa.s)
0.930	x	x	x	12.45	5.06	14.69	14.07	5.60	x	16.40	6.51	x
0.935	x	x	x	12.41	5.04	14.56	14.02	5.58	x	16.38	6.50	x
0.940	x	x	x	12.37	5.03	14.43	13.96	5.56	x	16.35	6.48	x
0.945	x	x	x	12.33	5.01	14.30	13.90	5.54	x	16.32	6.47	x
0.950	x	x	x	12.30	4.99	14.17	13.84	5.52	x	16.29	6.46	13.71
0.955	x	x	x	12.26	4.98	14.04	13.78	5.50	x	16.26	6.45	13.61
0.960	x	x	x	12.23	4.97	13.91	13.72	5.48	x	16.23	6.43	13.51
0.965	x	x	x	12.19	4.95	13.78	13.65	5.46	x	16.19	6.41	13.40
0.970	9.65	3.87	13.71	12.15	4.93	13.65	13.58	5.44	13.10	16.15	6.40	13.29
0.973	9.60	3.86	13.51	12.13	4.92	13.57	13.54	5.43	13.02	16.13	6.39	13.22
0.976	9.54	3.85	13.32	12.11	4.91	13.49	13.50	5.42	12.94	16.10	6.38	13.15
0.979	9.49	3.83	13.13	12.09	4.90	13.41	13.45	5.41	12.86	16.08	6.38	13.08
0.982	9.43	3.82	12.94	12.07	4.88	13.34	13.41	5.40	12.78	16.05	6.37	13.00
0.985	9.36	3.80	12.74	12.05	4.87	13.26	13.36	5.38	12.69	16.03	6.36	12.93
0.988	9.30	3.78	12.55	12.03	4.86	13.18	13.32	5.37	12.61	16.00	6.35	12.85
0.991	9.23	3.76	12.36	12.00	4.85	13.10	13.27	5.36	12.53	15.97	6.34	12.78
0.994	9.16	3.71	12.17	11.98	4.83	13.02	13.22	5.35	12.45	15.94	6.32	12.70
0.997	9.09	3.71	11.97	11.96	4.82	12.95	13.18	5.33	12.37	15.90	6.31	12.62
1.000	**9.00**	**3.67**	**11.78**	**11.88**	**4.81**	**12.87**	**13.00**	**5.30**	**12.29**	**15.89**	**6.30**	**12.54**
1.003	8.89	3.60	11.59	11.84	4.80	12.79	12.94	5.27	12.21	15.84	6.29	12.46
1.006	8.77	3.51	11.40	11.81	4.78	12.71	12.88	5.24	12.13	15.78	6.27	12.38
1.009	8.65	3.40	11.20	11.77	4.77	12.64	12.82	5.22	12.06	15.73	6.26	12.30
1.012	8.52	3.27	11.01	11.74	4.75	12.56	12.75	5.19	11.98	15.68	6.25	12.21
1.015	8.39	3.12	10.82	11.70	4.74	12.48	12.69	5.16	11.90	15.62	6.23	12.13
1.018	8.25	2.97	10.63	11.66	4.73	12.40	12.63	5.14	11.82	15.57	6.22	12.05
1.021	8.11	2.81	10.43	11.63	4.71	12.33	12.57	5.11	11.74	15.52	6.20	11.96
1.024	7.96	2.65	10.24	11.59	4.70	12.25	12.51	5.09	11.67	15.46	6.19	11.88
1.027	7.80	2.50	10.05	11.55	4.68	12.17	12.46	5.06	11.59	15.41	6.17	11.79
1.030	7.65	2.36	9.85	11.51	4.67	12.09	12.40	5.04	11.52	15.35	6.15	11.71
1.033	7.48	2.22	9.66	11.47	4.65	12.02	12.34	5.01	11.44	15.30	6.14	11.62
1.040	x	x	9.21	11.37	4.61	11.84	12.21	4.96	11.26	15.17	6.09	11.42
1.060	x	x	x	11.08	4.50	11.32	11.84	4.80	10.77	14.78	5.96	10.85
1.080	x	x	x	10.76	4.38	10.81	11.50	4.65	10.30	14.38	5.81	10.30
1.100	x	x	x	x	x	10.30	11.17	4.51	9.84	13.96	5.64	9.79
1.120	x	x	x	x	x	9.79	x	x	9.40	x	x	9.33
1.140	x	x	x	x	x	9.28	x	x	8.97	x	x	8.95
1.160	x	x	x	x	x	x	x	x	8.56	x	x	8.66

TABLE II. Elastic properties of Ge_xSe_{1-x} glasses. [1)]From Differential Scanning Calorimetry; [2)]Transition temperature observed in the E(T) measurement with the resonant technique. [3)]Softening rates measured in the supercooled-liquid range.

Glass	T_g [1)] (K)	T_g [2)] (K)	E_{RT} (GPa)	μ_{RT} (GPa)	ν_{RT}	$E(T_g)$ (GPa)	$\mu(T_g)$ (GPa)	$dE/dT(T_g^+)$ [3)] ($MPa.K^{-1}$)	$d\mu/dT(T_g^+)$ [3)] ($MPa.K^{-1}$)
a-Se	313	302	10.3	3.88	0.322	9.0	3.67	-115	-93.8
$GeSe_4$	435	416	14.73	5.73	0.286	11.8	4.81	-35.7	-14.3
$GeSe_3$	501	498	16.1	6.26	0.281	13.0	5.30	-38.4	-16.3
Ge_3Se_7	573	579	17.9	7.08	0.264	15.9	6.30	-30.8	-11.3

TABLE III. Viscous flow properties in the transition range of Ge_xSe_{1-x} glasses. [1)]Temperature for $\eta=10^{12}$ Pa.s; [2)]As defined by $m=d\log_{10}\eta/d(T(\eta=10^{12}\ Pa.s)/T)=\Delta H_a/(2.303RT_g)$ [43]; and [3)] ΔG_a measured near T_g, From the approach proposed by Nemilov [33,34]. nd: non-determined.

Glass	T_g [1)] (K)	ΔH_a (Eq.(6)) ($kJ.mol^{-1}$)	ΔG_a (Eq.(7)) ($kJ.mol^{-1}$)	ΔS_a (Eq.(8)) ($J.K^{-1}.mol^{-1}$)	m [2)]	ΔG_a [3)] ($kJ.mol^{-1}$)	ΔS_a [3)] ($J.K^{-1}.mol^{-1}$)	V^* [3)] ($m^3.mol^{-1}$)
a-Se	301	369	41	977	62	95	910	11.10^{-6}
$GeSe_9$	356	249	nd	nd	36	112	383	nd
$GeSe_4$	430	243	102	328	30	136	249	21.10^{-6}
$GeSe_3$	492	256	107	303	27	155	204	20.10^{-6}
Ge_3Se_7	580	294	145	160	27	183	191	23.10^{-6}

Figure captions:

FIG. 1a: Temperature dependence of Young's modulus (E).

FIG. 1b: Temperature dependence of the shear modulus (μ). Note the rapid decrease of the shear modulus in a-Se for T>Tg, which contrasts with the decrease found for E.

FIG. 2a: Temperature dependence of the shear viscosity coefficient (η)

FIG. 2b: Determination of the apparent activation energy (ΔH_a) from the viscosity data.

FIG. 3: Temperature dependence of Poisson's ratio (note that temperature is normalized to T_g as estimated from the E(T) data)

FIG. 4: T_g-scaled logarithm of viscosity from which the fragility index is straightforwardly derived from the slope of the linear intercepts in the transition range. The scaling parameter used here is the temperature corresponding to a viscosity of 10^{12} Pa.s.

FIG. 5: Activation entropy as calculated from Eq. (7) accompanying the shear viscous flow process in the transition range for glasses with different degrees of network cross-linking.

FIG. 6: Schematic drawing illustrating the thermally induced changes and the consequences on the elastic and viscous behaviors. Dashed lines show transverse load bearing arms, which oppose lateral contraction upon pulling along a vertical axis. Solid lines show possible regions for easy shear slip. The loading axis has to be imagined vertical in the plane of the figure. a) to d): a-Se, with increasing temperature. e) and f): Ge_xSe_{1-x} glasses with increasing germanium content for $x<0.2$. g) and h) at high germanium content ($x\geq0.20$), at rest and under stress.

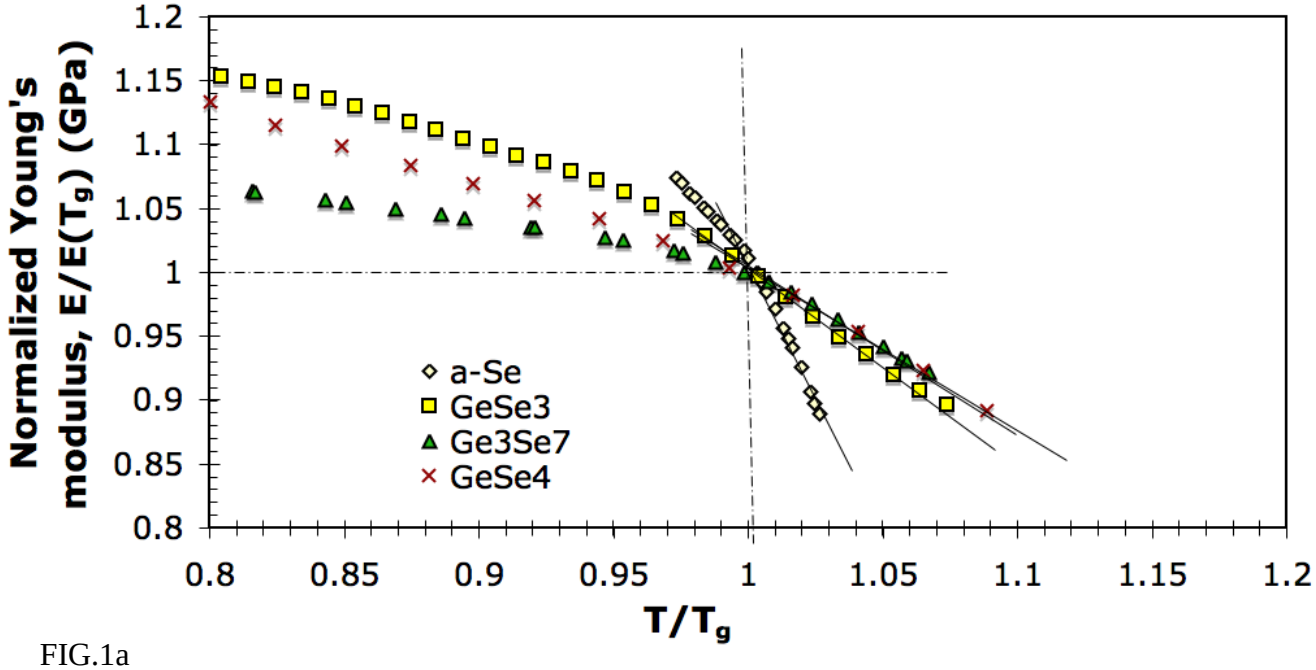
Normalized Young's modulus, E/E(Tg) (GPa)
T/Tg
a-Se
GeSe3
Ge3Se7
GeSe4
1.2
1.15
1.1
1.05
1
0.95
0.9
0.85
0.8
0.8
0.85
0.9
0.95
1
1.05
1.1
1.15
1.2

FIG.1a

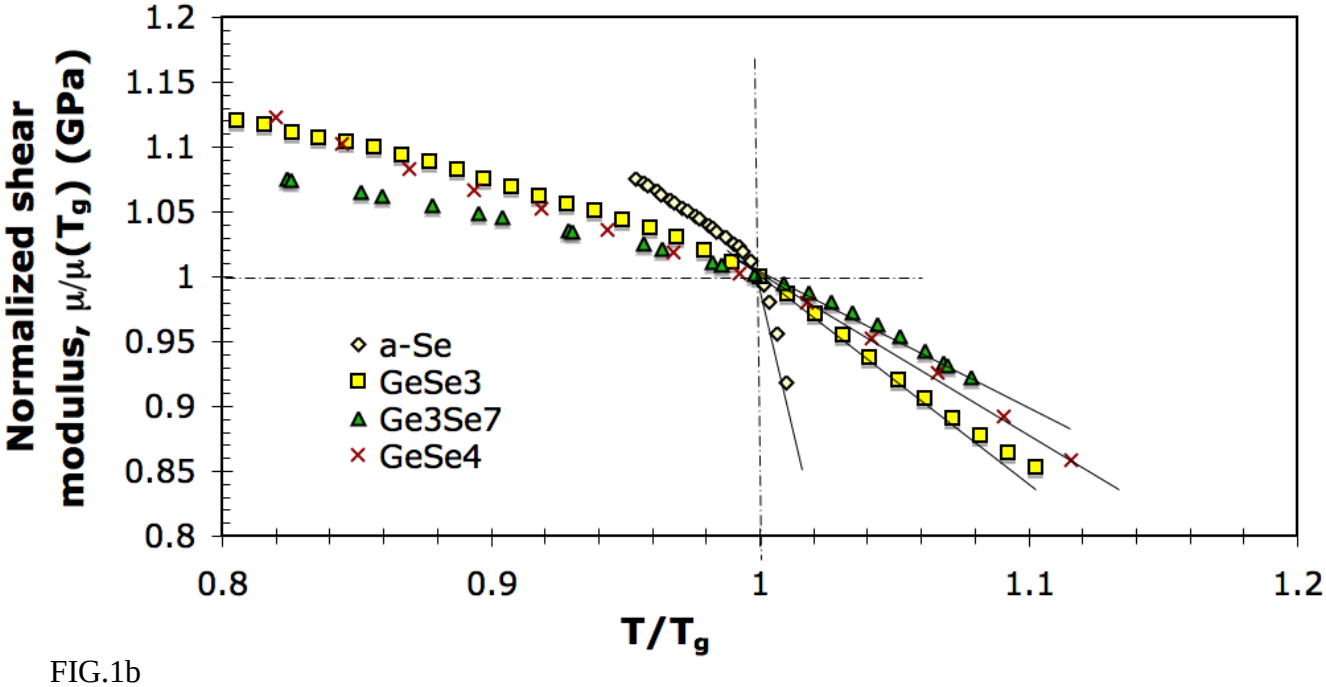
Normalized shear modulus, μ/μ(Tg) (GPa)
T/Tg
a-Se
GeSe3
Ge3Se7
GeSe4
1.2
1.15
1.1
1.05
1
0.95
0.9
0.85
0.8
0.8
0.9
1
1.1
1.2

FIG.1b

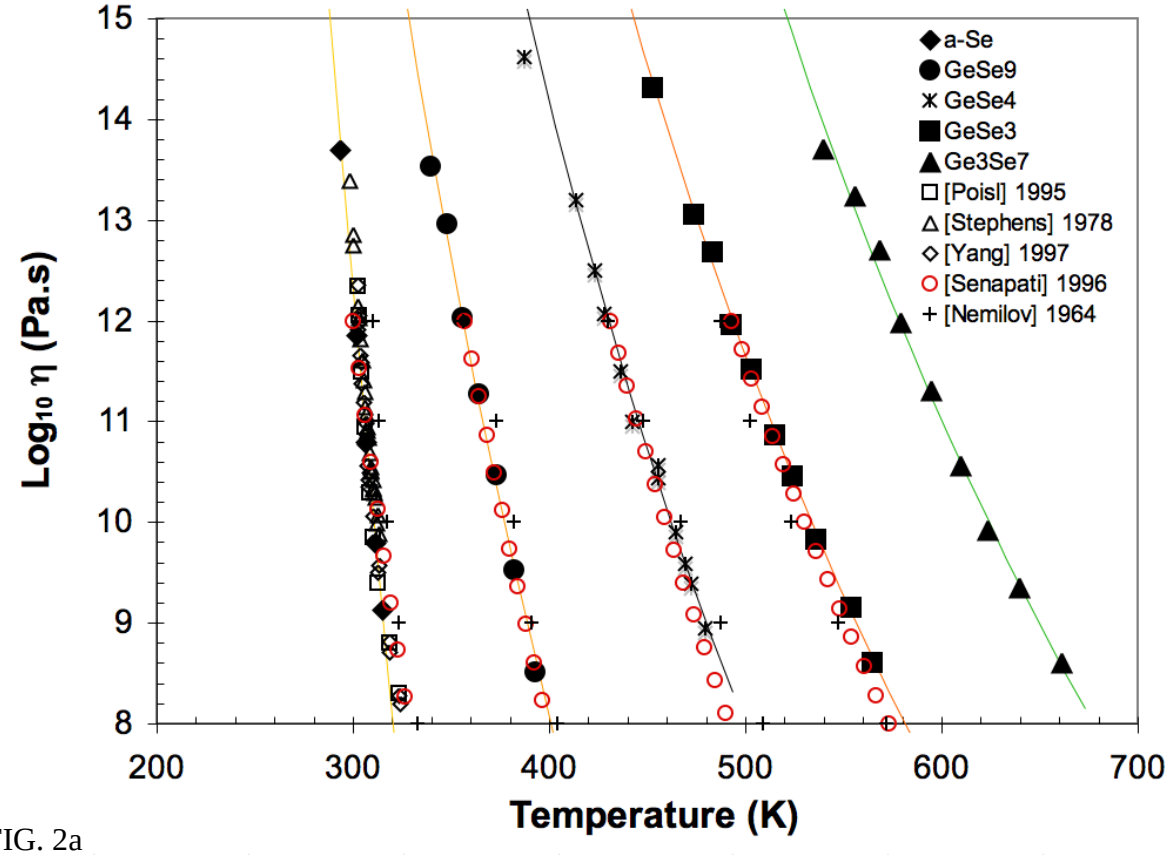
Log₁₀ η (Pa.s)
Temperature (K)
a-Se
GeSe9
GeSe4
GeSe3
Ge3Se7
[Poisl] 1995
[Stephens] 1978
[Yang] 1997
[Senapati] 1996
[Nemilov] 1964

FIG. 2a

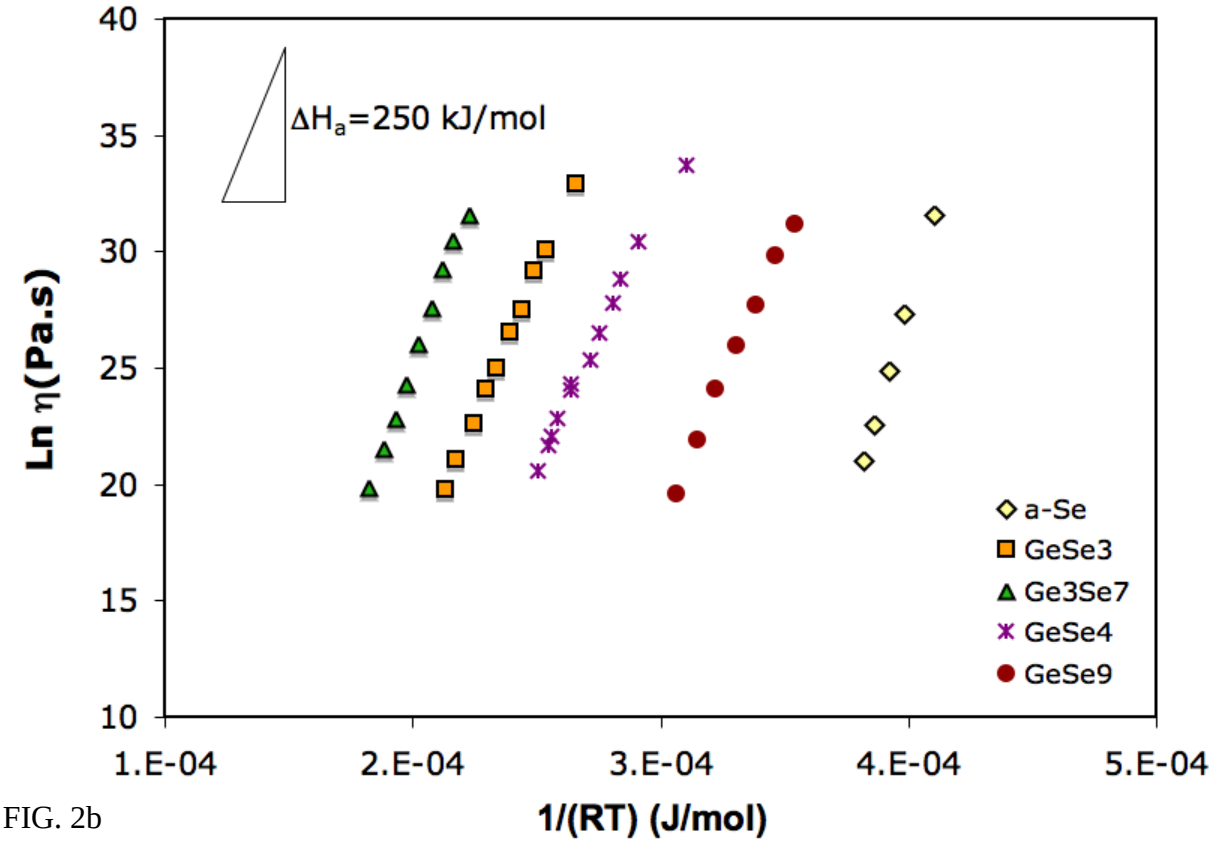
ΔHa=250 kJ/mol
Ln η(Pa.s)
1/(RT) (J/mol)
a-Se
GeSe3
Ge3Se7
GeSe4
GeSe9

FIG. 2b

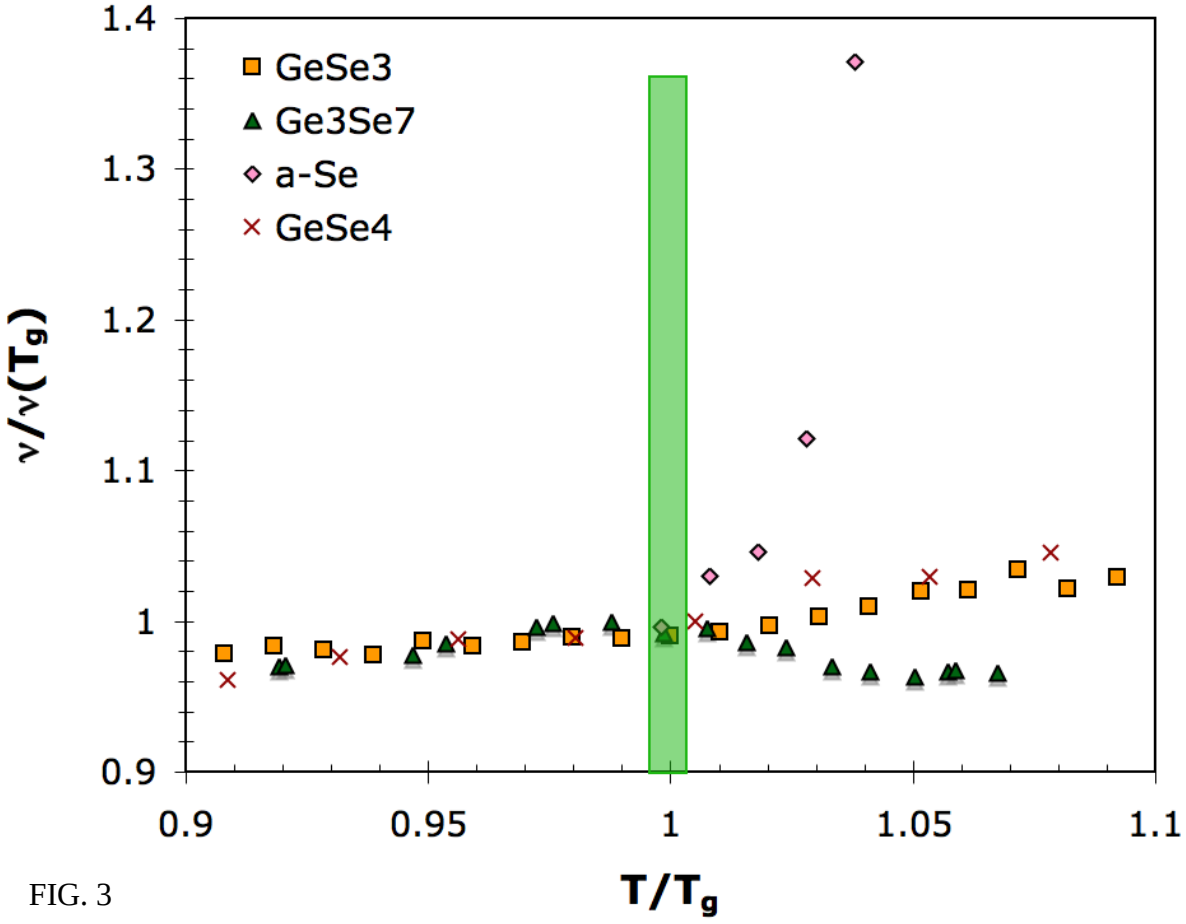
GeSe3
Ge3Se7
a-Se
GeSe4
ν/ν(Tg)
T/Tg
1.4
1.3
1.2
1.1
1
0.9
0.9
0.95
1
1.05
1.1

FIG. 3

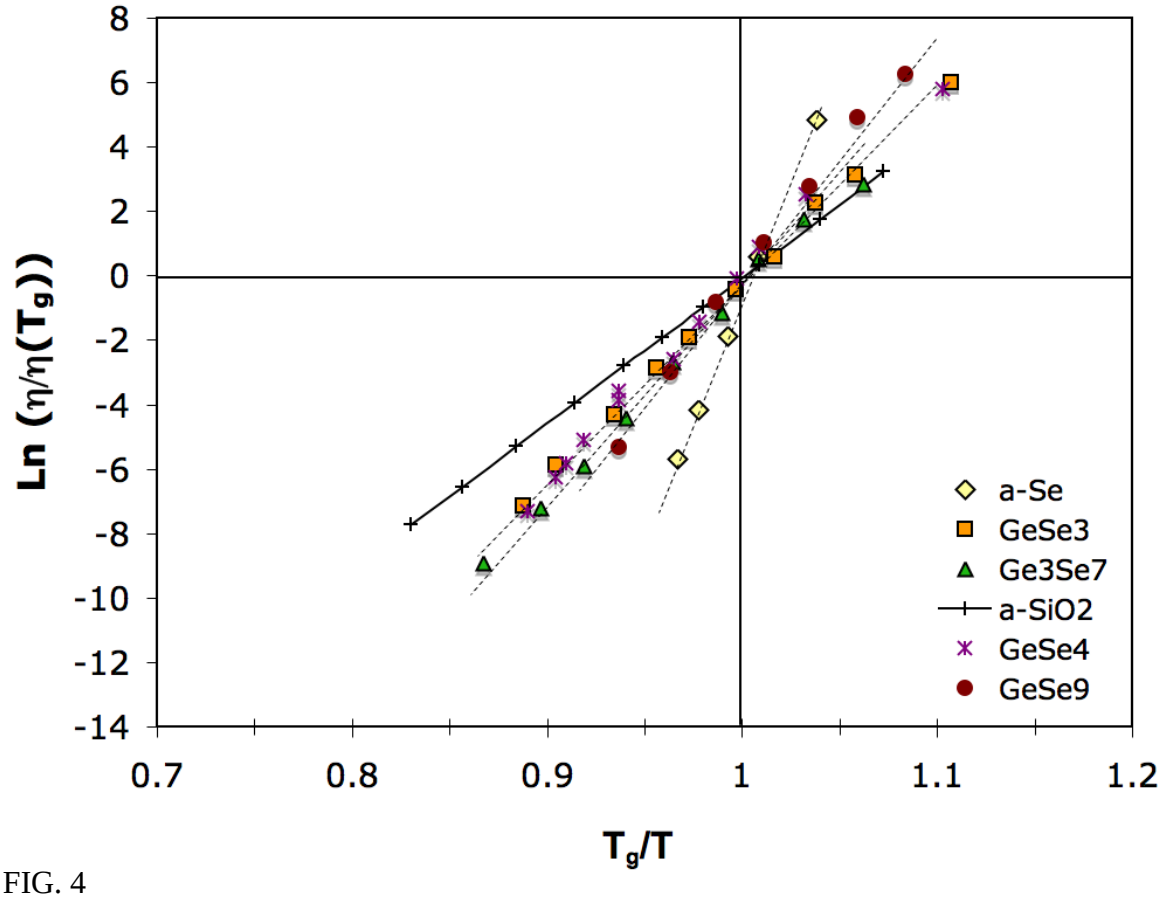
Ln (η/η(Tg))
Tg/T
8
6
4
2
0
-2
-4
-6
-8
-10
-12
-14
0.7
0.8
0.9
1
1.1
1.2
a-Se
GeSe3
Ge3Se7
a-SiO2
GeSe4
GeSe9

FIG. 4

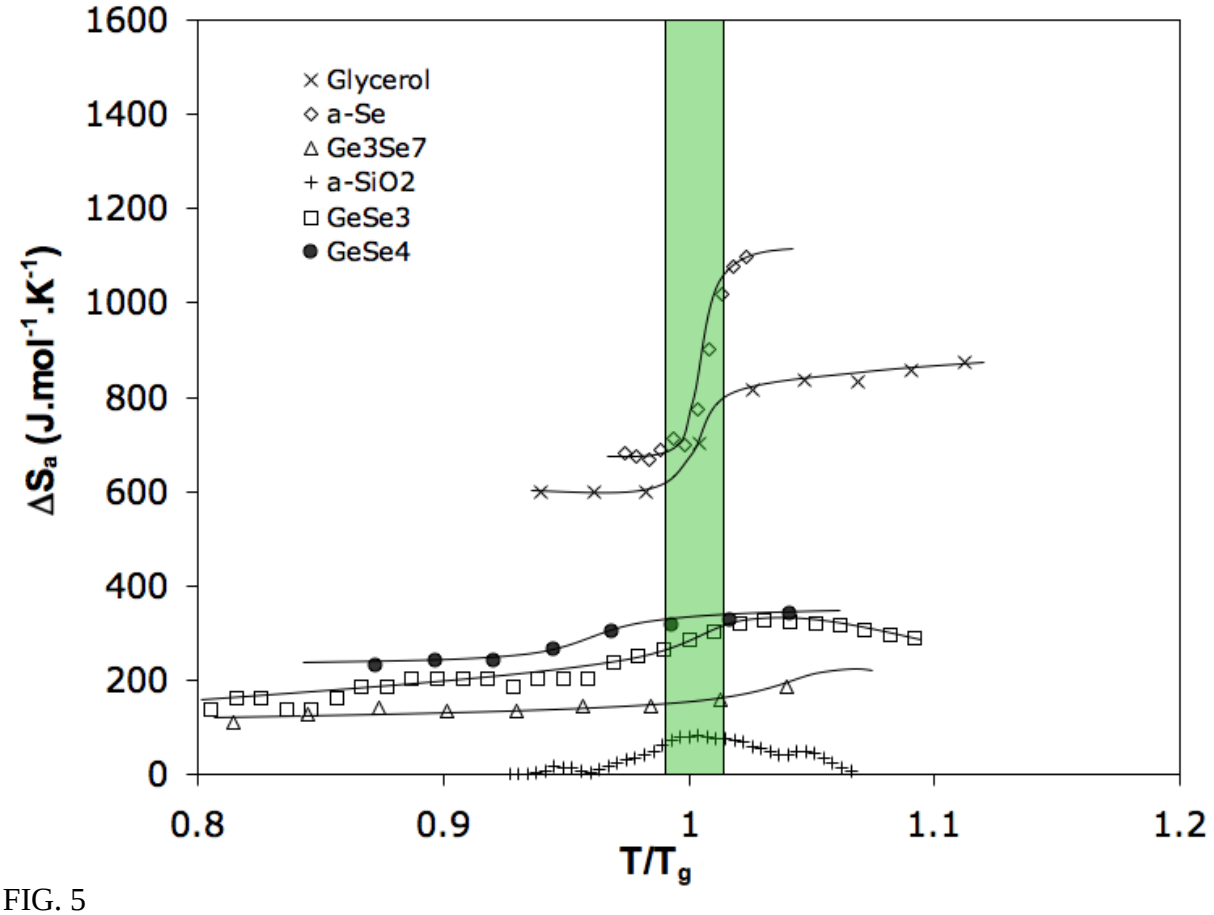
Glycerol
a-Se
Ge3Se7
a-SiO2
GeSe3
GeSe4
ΔSa (J.mol-1.K-1)
T/Tg
1600
1400
1200
1000
800
600
400
200
0
0.8
0.9
1
1.1
1.2

FIG. 5

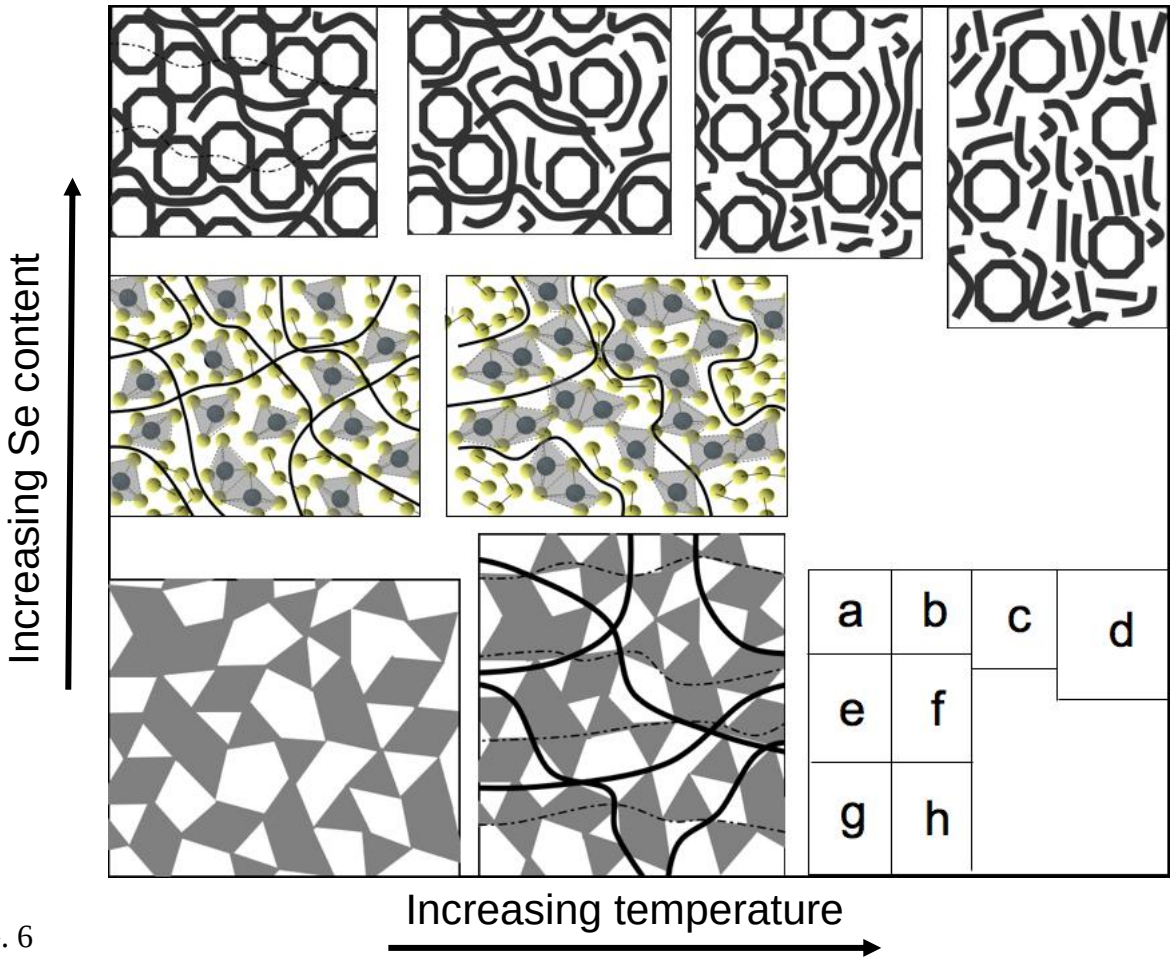
Increasing Se content
Increasing temperature
a
b
c
d
e
f
g
h

FIG. 6